THE ASTROPHYSICAL JOURNAL, 416:L33–L36, 1993 October 10

REFRIGERATION OF THE 18.3 GHz C_3H_2 TRANSITION IN DARK CLOUD G1.6−0.25

T. B. H. KUIPER,[1] J. B. WHITEOAK,[2] R.-S. PENG,[3] W. L. PETERS III,[4] AND J. E. REYNOLDS[2]

Received 1993 April 23; accepted 1993 July 30

ABSTRACT

We have observed 1_{10}–1_{01} (18.3 GHz) transition of ortho-cyclopropenylidene, C_3H_2, at 24 positions in the unusual dense cloud G1.6−0.025. Except for one position, the transition is refrigerated, a phenomenon which has not been seen in this transition before and was not predicted to occur. In general, the absorption correlates with the absorption seen in the 2_0–3_{-1} (12.2 GHz) transition of methanol, but there are significant differences. We suspect that collisional excitation at relatively high kinetic temperature (50 K) enhanced by photon trapping is responsible for the refrigeration.

Subject headings: ISM: individual (G1.6−0.025) — ISM: molecules — line: formation — molecular processes — radio lines: ISM

1. INTRODUCTION

Because of its relatively high abundance ($\sim 10^{-8}$) and large dipole moment (3.4 D), cyclopropenylidene (C_3H_2) is observed in a wide variety of molecular clouds. The carbon atoms form a triangle, with hydrogen atoms in the same plane attached to two of the carbons. As in H_2O, the spin statistics of the two off-axis hydrogen nuclei result in ortho and para symmetry species. Because, like H_2O, it has no symmetry of rotation, the resulting complex rotational energy level structures for both species lead to ample opportunities for anomalous population ratios under appropriate physical conditions. Such behavior was predicted (Avery 1987; Avery & Green 1989). The 2_{20}–2_{11} (21587 MHz) transition of para–C_3H_2, for example, is generobserved to be in absorption against the cosmic background radiation (e.g., Cox, Walmsley, & Güsten 1989; Madden et al. 1989).

Collisional excitation rates were computed by Green, DeFrees, & McLean (1987) for a kinetic temperature of 60 K and by Avery & Green (1989) for 10, 20, and 30 K. Statistical equilibrium calculations for 10 and 30 K using these rates predicted that the 1_{10}–1_{01} (18343 MHz) transition of ortho–C_3H_2 (see Fig. 1) occurs only in emission (Avery & Green 1989), and observations to date have supported that prediction.[5]

G1.6−0.025 is a warm (50 K) (Gardner et al. 1985), massive ($\sim 2 \times 10^6\ M_\odot$) (Whiteoak & Peng 1989) cloud with no associated continuum emission and few signs of star formation. It was first recognized to be a distinctive cloud for having an unusually wide absorption feature in H_2CO, centered at 50 km s^{-1} (Whiteoak & Gardner 1979). Subsequently, an unpublished southern ammonia survey (Peters et al. 1986, 1987) showed the cloud to have a very high optical depth, as deduced from the ratio of the satellite to the main hyperfine components. Gardner et al. (1985) mapped the cloud in several NH_3 transitions with the Parkes 64 m antenna and found that it had an overall extent of 10′ and a kinetic temperature above 50 K. There are several concentrations of high optical depth. Gardner & Boes (1987) found, in addition to the main emission at 50 km s^{-1}, emission at 150 km s^{-1} with a rotational temperature of 120 K.

Whiteoak & Peng (1989) found that the 2_0–3_{-1} (12.2 GHz) transition of methanol (CH_3OH) absorbs the background radiation much more strongly in this source than in any other. Since the background emission at 12 GHz was estimated from the results compiled by Downes & Maxwell (1966) to be about 0.25 K, and the peak absorption is 2.0 K, it is clear that the transition is refrigerated with an excitation temperature of less than 1 K. Peng & Whiteoak (1993) derived an excitation temperature of 0.4 K. Thus, the cloud is a Class I methanol source (Menten 1991; formerly called class A—see Batrla et al. 1987), which is to say, a source in which methanol is excited primarily by collisions (Walmsley et al. 1988). This type of excitation normally occurs in cool dense clouds. This classification is confirmed by the observations of the 4_{-1}–3_0 (36.2 GHz) transitions (Berulis et al. 1992; Haschick & Baan 1993). Consideration of the excitation mechanism suggested to Sobolev (1992) that the 150 km s^{-1} cloud and the 50 km s^{-1} cloud are colliding. Because of the accurate superposition of one of the 50 km s^{-1} maxima at 36.2 GHz on the 150 km s^{-1} maximum, the occurrence of methanol masers at both velocities, and the enhanced gas temperatures, Haschick & Baan (1993) supported this conclusion. On the basis of statistical equilibrium calculations, Peng & Whiteoak (1993) conclude that the strong absorption is due to nondominating collisional excitation at warm ($T_K \geq 30$ K) gas temperatures.

Adding to the unusual properties of this source, we here report the first observation of refrigeration in the 18.3 GHz ground-state transition of ortho–C_3H_2 in a dark cloud.

2. OBSERVATIONS

The observations were made between 1991 April 21 and 1993 February 7 with the NASA Deep Space Network 70 m

[1] Jet Propulsion Laboratory, 169-506, California Institute of Technology, Pasadena, CA 91109. E-mail: I: kuiper@dsnra.jpl.nasa.gov.
[2] Australia Telescope National Facility, Commonwealth Scientific and Industrial Research Organization, P.O. Box 76, Epping, NSW 2121, Australia. E-mail: I: jreynold@atnf.csiro.au, jwhiteoa@atnf.csiro.au.
[3] School of Physics, University of New South Wales, Kensington, NSW 2033, Australia. Current address: Department of Astronomy, University of Illinois at Urbana-Champaign, 1002 West Green Street, Urbana, IL 61801. E-mail: I: peng@submm.astro.uiuc.edu.
[4] Steward Observatory, University of Arizona, Tucson, AZ 85721. E-mail: I: wpeters@as.arizona.edu.
[5] In his first statistical equilibrium calculations, Avery (1987) had found that the 18343 MHz transition would absorb the cosmic background radiation below densities of about $10^{4.5}$–10^5 cm^{-3} and at a kinetic temperature of 10 K, but these calculations used H_2O-He collisional cross sections, scaled by a factor of 10 as an approximation, which bear little resemblance to the rates calculated later.

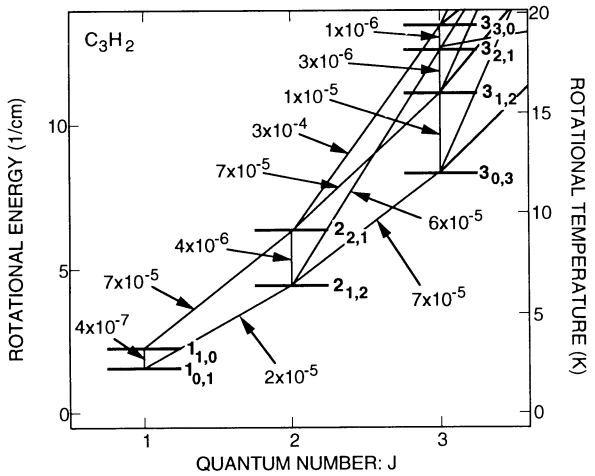

FIG. 1.—Lower part of the energy level diagram of ortho-C_3H_2, showing the main radiative transitions.

antenna in Canberra, Australia. At 18.3 GHz, the antenna has a peak aperture efficiency of 0.55 and a beamwidth of 55″. The low-noise preamplifier consists of a cooled–high electron mobility transistor 12–18 GHz amplifier built by the US National Radio Astronomy Observatory in a front-end package originally built by Haystack Observatory. Since the system was operated beyond its design limit, the system temperature at the zenith in clear weather was typically 90–120 K. Postamplification and down-conversion to an intermediate frequency of 321.4 MHz were done with a Hewlett-Packard Modular Measurement System, which was locked to the station's hydrogen-maser frequency reference system. A digital Fourier transform spectrometer with 256 channels and a maximum bandwidth of 10 MHz was used.

Spectra of the 50 km s^{-1} feature were obtained at 24 positions using position-switching and a 10 MHz bandwidth (corresponding to 164 km s^{-1}, with 0.64 km s^{-1} between channels). To be sure that the absorption was not an artifact due to emission at the off position, several off positions were used. The results were found not to depend on the choice of off position. The antenna temperatures were converted to brightness temperatures using a model of beam efficiency as a function of elevation. The spectra had quadratic baselines removed and were fitted to Gaussians. The parameters of the fits, the standard deviation of the data, and the off positions used are tabulated in Table 1. The positions are given in arcminutes of right ascension and declination relative to $17^h46^m12^s$, $-27°33'12''$ (1950.0). Figure 2 shows the spectra at three positions. We accumulated the most integration time at position (0, 0), 2800 s total on-source and off-source.

A search was also made for the 150 km s^{-1} feature at the (0, 0) position, and an upper limit of 0.05 K was obtained.

3. ANALYSIS

The size of the cloud in relation to our beam and the weak signal strength made it impractical to map the cloud in reasonable time, and we were constrained to sample regions of particular interest.

If the 18.3 GHz C_3H_2 absorption depends mainly on C_3H_2 column density, then, as the 12.2 GHz CH_3OH absorption appears to follow column density (Whiteoak & Peng 1989), there should be a correlation between the two lines. In the central region of the cloud, the absorption observed in the 18.3 GHz C_3H_2 line behaves similarly to the absorption in the 12.2 GHz CH_3OH line but with distinct differences. For example, at the (0, 0) position, the C_3H_2 line peaks at 62 km s^{-1}, whereas the CH_3OH line peaks at 50 km s^{-1} (see Fig. 1 in Whiteoak & Peng 1989), but the widths are about the same (18 vs. 21 km s^{-1}). Some of this difference may be due to the disparate beam sizes used: 2′ for CH_3OH versus 55″ for C_3H_2. In Figure 3 we plot the fitted peak brightness temperatures (T_B) in the C_3H_2 transition against methanol fitted peak T_B, which

TABLE 1

SUMMARY OF OBSERVATIONS

Position (arcminutes)	T_B (K)	V_{LSR} (km s^{-1})	ΔV (km s^{-1})	RMS (K)	Off Position (R.A., decl.)	
4E	−0.16 ± 0.01	53.8 ± 0.6	12.9 ± 1.4	0.05	−1?0	0?0
4E1S	−0.22 ± 0.02	53.3 ± 1.0	10.9 ± 2.3	0.08	−1.0	0.0
3E	−0.20 ± 0.02	53.4 ± 0.7	12.9 ± 1.6	0.06	−1.0	0.0
2E2N	−0.20 ± 0.02	51.6 ± 0.6	13.2 ± 1.4	0.06	−1.0	0.0
2E1N	−0.24 ± 0.02	49.1 ± 0.5	15.9 ± 1.2	0.06	−1.0	0.0
2E	−0.17 ± 0.01	54.1 ± 0.6	16.9 ± 1.3	0.04	±1.0	0.0
2E1S	−0.21 ± 0.02	53.9 ± 0.5	13.2 ± 1.1	0.05	−1.0	0.0
1E1N	−0.24 ± 0.02	50.1 ± 0.6	10.8 ± 1.3	0.07	−1.0	0.0
1E	−0.19 ± 0.01	53.3 ± 0.8	21.8 ± 1.8	0.05	+1.0	0.0
1E1S	−0.25 ± 0.02	53.1 ± 0.5	14.4 ± 1.1	0.06	−1.0	0.0
0.5E	−0.22 ± 0.01	55.9 ± 0.7	21.9 ± 1.7	0.06	+1.0	0.0
1N	−0.12 ± 0.02	55.6 ± 1.1	21.1 ± 2.5	0.06	+1.0	0.0
CENTER	−0.21 ± 0.01	61.7 ± 0.5	18.2 ± 1.1	0.04	±1.0	0.0
1S	−0.20 ± 0.01	53.8 ± 0.8	20.0 ± 1.8	0.06	+1.0	0.0
4S	−0.18 ± 0.04	58.4 ± 1.2	10.2 ± 2.9	0.12	+2.0	−2.0
0.5W	−0.32 ± 0.02	60.9 ± 0.5	18.9 ± 1.3	0.07	+1.0	0.0
1WIN	−0.15 ± 0.03	52.9 ± 1.3	12.1 ± 3.1	0.09	−1.0	0.0
1W	−0.21 ± 0.02	65.1 ± 0.9	24.7 ± 2.2	0.07	+1.0	0.0
1W1S	−0.24 ± 0.02	60.9 ± 0.8	17.9 ± 1.8	0.08	−1.0	0.0
2W	−0.23 ± 0.02	65.2 ± 0.9	26.5 ± 2.2	0.07	+1.0	0.0
4W2N	−0.09 ± 0.02	45.1 ± 0.9	8.1 ± 2.1	0.04	+2.0	−2.0
3W	−0.13 ± 0.02	77.2 ± 1.6	20.9 ± 3.8	0.09	+1.0	0.0
4W4S	−0.13 ± 0.02	53.5 ± 2.5	27.9 ± 6.0	0.11	+2.0	−2.0
4W8S	+0.04 ± 0.01	65.9 ± 1.6	11.9 ± 3.9	0.04	+2.0	−2.0

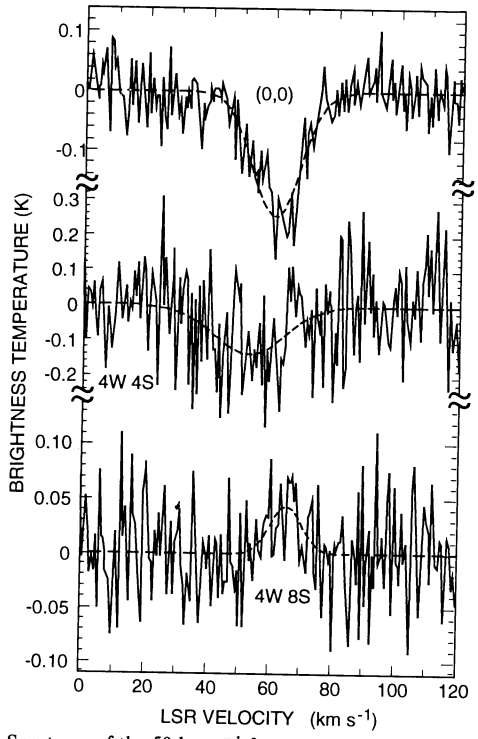

FIG. 2.—Spectrum of the 50 km s^{-1} feature at positions (0, 0), 4W4S, and 4W8S relative to $17^h46^m12^s$, −27°33′12″ (1950.0).

were obtained by interpolating Fig. 2 of Whiteoak & Peng (1989). We fitted a straight line to the data, which is shown as a dashed line in the figure. (In doing the fit, we used as a measure of the error in T_B one-quarter of the standard deviation, because the values returned by the data reduction program for the T_B error did not have enough significant digits.) We see that, in general, there is a correlation, but the data are scattered rather widely about the fitted line. This suggests that there are differences between the spatial structure in the C_3H_2 absorption and the CH_3OH absorption. An explanation for this could be that refrigeration of the 18.3 GHz C_3H_2 transition is more sensitive to physical conditions than the 12.2 GHz CH_3OH transition.

At the 4W8S position, weak emission is seen at 65 km s^{-1} (Fig. 2). (This point was therefore not included in the fit of the data in Fig. 3.) This suggests that the conditions which cause

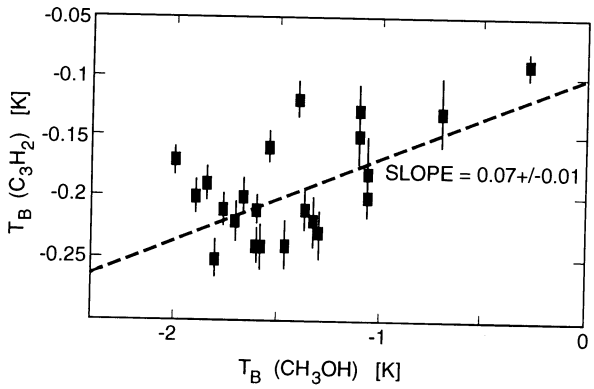

FIG. 3.—18.3 GHz C_3H_2 absorption plotted against 12.2 GHz CH_3OH absorption. The emission (*open circle*) was not included in the regression.

refrigeration in this transition no longer occur as one moves toward or beyond the periphery of the cloud. This can be contrasted with the behavior of the 12 GHz CH_3OH transition, which has never been observed in emission in dark clouds. If the cloud edges show profiles with a mixture of absorption and emission and there is a velocity gradient across the cloud, such as we observe, then there will be a departure from the general velocity correlation seen in the inner part of the cloud. As an example of this, the 4W4S position may have a relatively narrow (~7 km s^{-1}) emission feature at 70 km s^{-1} filling in the wing of an absorption feature (Fig. 2) which, from the methanol data, is expected to occur at 60 km s^{-1}.

Velocity variation along the line of sight, combined with emission from the cloud edges, will also affect profiles measured near the cloud center. We correlated the LSR velocities and line widths but excluded the data taken at positions 4W8S, 4W4S, and 4W2N for the reason given above. The C_3H_2 velocities cover a wider range than those of methanol (slope = 2.0 ± 0.1) and are scattered quite widely about the best fit. The line width data also show considerable scatter nevertheless, with a weak correlation (0.75 ± 0.12) between the C_3H_2 line widths and the methanol line widths.

4. DISCUSSION

The question to be resolved is what combination of physical conditions in G1.6−0.025 gives rise to the refrigeration of the 18.3 GHz C_3H_2 transition. The phenomenon is certainly unusual. It was the single case detected during a survey which included 144 positions in 72 southern dark clouds. (However, absorption of continuum emission by this transition is quite common.) Furthermore, 49 additional northern dark clouds have been surveyed by Cox et al. (1989) and Madden et al. (1989). (There are 13 positions in common in these two surveys.) Also, the variability of the C_3H_2 profiles compared to the rather smoothly varying CH_3OH profiles suggests that the C_3H_2 excitation is acutely sensitive to some special combination of conditions.

The density of G1.6−0.025, ~10^4 cm^{-3} (Peng & Whiteoak 1993), does not appear to be unusual. The cloud is unusual in having a high H_2 column density (2 × 10^{23}–10^{24} cm^{-3}; Whiteoak & Peng 1989) and high temperature (~50 K; Gardner & Boes 1987) but no strong embedded infrared sources which are responsible for the heating.

Nondominating (i.e., at densities < 10^8 cm^{-3}) collisional excitation at relatively high kinetic temperature, possibly enhanced by photon trapping, may be responsible for the refrigeration. This explanation is plausible on physical grounds because at higher temperatures, collisions from the $1_{1,0}$ (upper) level to the $2_{2,1}$ level become increasingly important for removing molecules from the $1_{1,0}$ state. In addition, spontaneous decays in the opposite direction may be inhibited by photon trapping resulting from high column density.

Figure 4 shows the excitation rates for collisions with helium atoms (Green et al. 1987; Avery & Green 1989). At low temperatures (10–30 K), the collisional transition rates out of the upper ($1_{1,0}$) level of the 18.3 GHz transition are about equal but four times lower than those out of the lower ($1_{0,1}$) level. However, at higher temperatures, $1_{1,0}$–$2_{2,1}$ collisional excitation becomes the path for depopulating the upper level, with a rate comparable to those for depopulating the lower level.

In Figure 1, the rate of spontaneous emission is shown next to the line representing the transition. The main pathway responsible for populating the upper ($1_{1,0}$) level of the 18.3

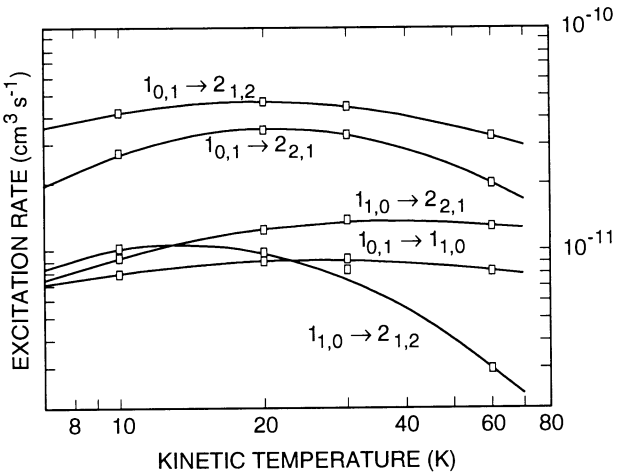

FIG. 4.—Excitation rates for collisions with He for the lower levels of ortho-C_3H_2. The open squares are the published rates.

GHz transition is radiative decay from the $2_{2,1}$ level. Note that the rate for spontaneous emission is three times higher for this pathway than for the pathway which populates the lower ($1_{0,1}$) level of the 18.3 GHz transition. Consequently, inhibition of this pathway could contribute to an underpopulation of the $1_{1,0}$ level. At first glance, this effect would not seem to be important. Assuming local thermodynamic equilibrium, a C_3H_2 abundance of 4×10^{-9} (Cox et al. 1989), an H_2 column density of 10^{24} cm^{-2}, a line width of 15 km s^{-1}, and a temperature of 50 K, the $2_{2,1}$–$1_{1,0}$ (122 GHz) transition has an optical depth of 0.2, which implies that photon trapping is unimportant. However, if the C_3H_2 abundance were somewhat greater, then the photon escape probability for the radiative decays into the upper level of the 18.3 GHz transition would be about 70% of the probability for the decays into the lower level. This could contribute to lowering the $1_{1,0}/1_{0,1}$ population ratio.

The question of whether either mechanism alone is sufficient to refrigerate the 18.3 GHz transition or the two need to act in concert must be answered by detailed modeling.

We noted a general correlation between the C_3H_2 18.3 GHz absorption and the corresponding CH_3OH 12.2 GHz absorption in G1.6−0.025. This shows that the amount of C_3H_2 absorption is generally dependent on the H_2 column density, which is traced out by the CH_3OH absorption. The lack of detailed correlation of the C_3H_2 profiles with the CH_3OH profiles is consistent with the detection of emission at the cloud boundary. If the conditions for refrigeration break down toward the edges of the cloud, perhaps because photon trapping is not effective there, then the observed profiles will represent a mixture of absorption and emission along the line of sight and at various LSR velocities, whereas CH_3OH shows only absorption.

In view of the general correlation between C_3H_2 and CH_3OH absorption at 50 km s^{-1}, our failure to detect the 150 km s^{-1} component in C_3H_2 could simply be due to lack of sensitivity, because in methanol this component is one-fifth as strong as the 50 km s^{-1} component. Thus, it would be a mere −0.05 K in the C_3H_2 transition, which is about the noise level of our data.

We gratefully acknowledge the assistance of the Director and staff of the Canberra Deep Space Communication Complex (Tidbinbilla). Part of this work was performed by the Jet Propulsion Laboratory, California Institute of Technology, under contract with the National Aeronautics and Space Administration.

REFERENCES

Avery, L. W. 1987, in IAU Symp. 120, Radio and Millimetre Observations of Larger Molecules ed. M. S. Vardya & S. P. Tarafdar (Dordrecht: Reidel), 187
Avery, L. W., & Green, S. 1989, ApJ, 337, 306
Batrla, W., Matthews, H. E., Menten, K. M., & Walmsley, C. M. 1987, Nature, 326, 49
Berulis, I. I., Kalenski, S. V., Sobolov, A. M., & Strelnitski, V. S. 1992, A&ATrans, 1, 231
Cox, P., Walmsley, C. M., & Güsten, R. 1989, A&A, 209, 382
Downes, D., & Maxwell, A. 1966, ApJ, 146, 653
Gardner, F. F., & Boes, F. 1987, Proc. Astron. Soc. Australia, 7, 185
Gardner, F. F., Whiteoak, J. B., Forster, J. R., Peters, W. L., & Kuiper, T. B. H. 1985, Proc. Astron. Soc. Australia, 6, 176
Green, S., DeFrees, D. J., & McLean, A. D. 1987, ApJS, 65, 175
Haschick, A. D., & Baan, W. A. 1993, ApJ, 410, 663
Madden, S. C., Irvine, W. M., Matthews, H. E., Friberg, P., & Swade, D. A. 1989, AJ, 97, 1403
Menten, K. M. 1991, in Atoms, Ions, and Molecules: New Results in Spectral Line Astrophysics, ed. A. D. Haschick & P. T. P. Ho (San Francisco: ASP), 119
Peng, R. S., & Whiteoak, J. B. 1993, MNRAS, 260, 529
Peters, W. L., Forster, J. R., Gardner, F. F., Whiteoak, J. B., & Kuiper, T. B. H. 1986, Proc. Astron. Soc. Australia, 6, 504
Peters, W. L. et al. 1987, in Star Forming Regions, ed. M. Peimbert & J. Jugaku (Dordrecht: Reidel), 66
Sobolev, A. M. 1992, preprint
Walmsley, C. M., Batrla, W., Matthews, H. E., & Menten, K. M. 1988, A&A, 197, 271
Whiteoak, J. B., & Gardner, F. F. 1979, MNRAS, 188, 445
Whiteoak, J. B., & Peng, R.-S. 1989, MNRAS, 239, 677